ORGANOMETALLICS
Article

Organometallics **2009,** *28,* 4979–4987 4979
DOI: 10.1021/om9005017

Syntheses, Structures, and Dynamic Properties of Dicobalt π Complexes of Diplatinum Polyynediyl Complexes

Helene Kuhn,[†] Frank Hampel,[†] and John A. Gladysz*[,‡]

[†]*Institut für Organische Chemie and Interdisciplinary Center for Molecular Materials, Friedrich-Alexander-Universität Erlangen-Nürnberg, Henkestrasse 42, 91054 Erlangen, Germany, and* [‡]*Department of Chemistry, Texas A&M University, P.O. Box 30012, College Station, Texas 77842-3012*

Received June 12, 2009

Reactions of $Co_2(CO)_6(\mu\text{-}Ph_2PCH_2PPh_2)$ and polyynediyl complexes *trans*,*trans*-(C_6F_5)-$(p\text{-}tol_3P)_2Pt(C{\equiv}C)_mPt)(P$*p*-$tol_3)_2(C_6F_5)$ (**PtC$_{2m}$Pt**) are conducted in refluxing toluene. With **PtC$_8$Pt**, a 1:1 adduct, *trans*,*trans*-$(C_6F_5)(p\text{-}tol_3P)_2PtC{\equiv}CC_2[Co_2(CO)_4(\mu\text{-}PPh_2CH_2PPh_2)](C{\equiv}C)_2Pt(P$*p*-$tol_3)_2(C_6F_5)$ (**1**), is isolated in 53% yield after silica gel chromatography and crystallographically characterized. The dicobalt moiety binds to a $PtC{\equiv}C\underline{C}{\equiv}\underline{C}$ linkage remote from the bulky platinum endgroups, with the P−Pt−P axis of the $(p\text{-}tol_3P)_2\underline{P}tC{\equiv}CC(Co)_2$ moiety nearly parallel to the cobalt−cobalt bond and that of the $(p\text{-}tol_3P)_2PPtC{\equiv}CC{\equiv}CC(Co)_2$ moiety roughly perpendicular. The ^{31}P and ^1H NMR spectra of **1** evidence dynamic behavior. At the low-temperature limit, three ^{31}P signals are observed (2:1:1), corresponding to the *p*-tol_3P ligands on one endgroup and those that have cis/trans relationships to the cobalt−cobalt bond on the other. Low-temperature ^{31}P and ^1H NMR spectra show multiple $Ph_2\underline{P}C\underline{H}_2\underline{P}Ph_2$ signals, which are analyzed. In the case of **PtC$_{12}$Pt**, a 2:1 adduct is the major isolable product (12%). NMR data show that the dicobalt moieties bind to the central C≡C linkages furthest from the endgroups. In the case of **PtC$_{16}$Pt**, mass spectra show that 2:1 adducts can form, but ^{31}P NMR spectra are not homogeneous, suggesting mixtures of isomers differing in the dicobalt positions.

Introduction

Over the past few years, there has been intense interest in the synthesis and detailed physical characterization of compounds with long sp carbon chains, i.e., those with four or more C≡C units (octatetraynediyl or C_8 species).[1−3] Compounds that can be isolated under ambient laboratory conditions now include several C_{20} adducts,[4−8] two C_{24} species, one of which features $-CCo_3$ endgroups,[8,9] and one C_{28} complex.[8] Other long-chain systems have proved spectroscopically detectable.[1] However, the development of the chemistry of the polyyne moiety has lagged.

One of the most general and characteristic organometallic reactions of alkynes would be their derivatization as $Co_2(CO)_6$ or $Co_2(CO)_4(L)_2$ adducts.[10] As documented in numerous crystal structures, these feature orthogonal C≡C and $(L)(CO)_2Co-Co(CO)_2(L)$ linkages, affording pseudotetrahedral Co_2C_2 cores.[10] Accordingly, a variety of conjugated polyynes have been treated with $Co_2(CO)_8$ or $Co_2(CO)_6(L)_2$ precursors. In particular, Bruce has reported the derivatization of a number of bimetallic polyynediyl complexes $L_nM(C{\equiv}C)_mML_n$ and related species, including several octatetraynediyl (MC_8M) compounds.[11,12] In some cases, it has proved possible to complex more than one C≡C unit, but mixtures of dicobalt and tetracobalt adducts are often obtained.[11a] In many cases, these are chromatographically separable. Further product diversity is suggested by the trace amounts of additional species frequently noted, but for

*To whom correspondence should be addressed. E-mail: gladysz@mail.chem.tamu.edu.

(1) Chalifoux, W. A.; Tykwinski, R. R. *C. R. Chim.* **2009**, *12*, 341.
(2) Szafert, S.; Gladysz, J. A. *Chem. Rev.* **2003**, *103*, 4175; 2006, 106, PR1−PR33.
(3) Bruce, M. I.; Low, P. J. *Adv. Organomet. Chem.* **2004**, *50*, 179.
(4) (a) Gibtner, T.; Hampel, F.; Gisselbrecht, J.-P.; Hirsch, A. *Chem.—Eur. J.* **2002**, *8*, 408. See also: (b) Klinger, C.; Vostrowsky, O.; Hirsch, A. *Eur. J. Org. Chem.* **2006**, 1508.
(5) (a) Eisler, S.; Slepkov, A. D.; Elliot, E.; Luu, T.; McDonald, R.; Hegmann, F. A.; Tykwinski, R. R. *J. Am. Chem. Soc.* **2005**, *127*, 2666. See also: (b) Luu, T.; Elliot, E.; Slepkov, A. D.; Eisler, S.; McDonald, R.; Hegmann, F. A.; Tykwinski, R. R. *Org. Lett.* **2005**, *7*, 51.
(6) Dembinski, R.; Bartik, T.; Bartik, B.; Jaeger, M.; Gladysz, J. A. *J. Am. Chem. Soc.* **2000**, *122*, 810.
(7) (a) Mohr, W.; Stahl, J.; Hampel, F.; Gladysz, J. A. *Chem.—Eur. J.* **2003**, *9*, 3324. (b) Kuhn, H.; Gladysz, J. A. Manuscript in preparation. (c) Kuhn, H. Doctoral dissertation, Universität Erlangen-Nürnberg, **2009**.
(8) (a) Zheng, Q.; Gladysz, J. A. *J. Am. Chem. Soc.* **2005**, *127*, 10508. (b) Zheng, Q.; Bohling, J. C.; Peters, T. B.; Frisch, A. C.; Hampel, F.; Gladysz, J. A. *Chem.—Eur. J.* **2006**, *12*, 6486.
(9) Bruce, M. I.; Zaitseva, N. N.; Nicholson, B. K.; Skelton, B. W.; White, A. H. *J. Organomet. Chem.* **2008**, *693*, 2887.
(10) Review literature: (a) Dickson, R. S.; Fraser, P. J. *Adv. Organomet. Chem.* **1974**, *12*, 323. (b) Kemmitt, R. D. W.; Russell, D. R. In *Comprehensive Organometallic Chemistry*; Wilkinson, G. W.; Stone, F. G. A.; Abel, E. W., Eds.; Pergamon: Oxford, 1982; Vol. *5*, Chapter 34.4.1.
(11) (a) Bruce, M. I.; Kelly, B. D.; Skelton, B. W.; White, A. H. *J. Chem. Soc., Dalton Trans.* **1999**, 847. (b) Bruce, M. I.; Kelly, B. D.; Skelton, B. W.; White, A. H. *J. Organomet. Chem.* **2000**, *604*, 150.
(12) (a) See also: Chung, M.-C.; Sakurai, A.; Akita, M.; Moro-oka, Y. *Organometallics* **1999**, *18*, 4684. (b) For the first crystallographically characterized dicobalt π complex of a polyynediyl complex, see: Akita, M.; Sakurai, A.; Moro-oka, Y. *Chem. Commun.* **1999**, 101.

Published on Web 08/04/2009

Scheme 1. Syntheses of the Title Compounds

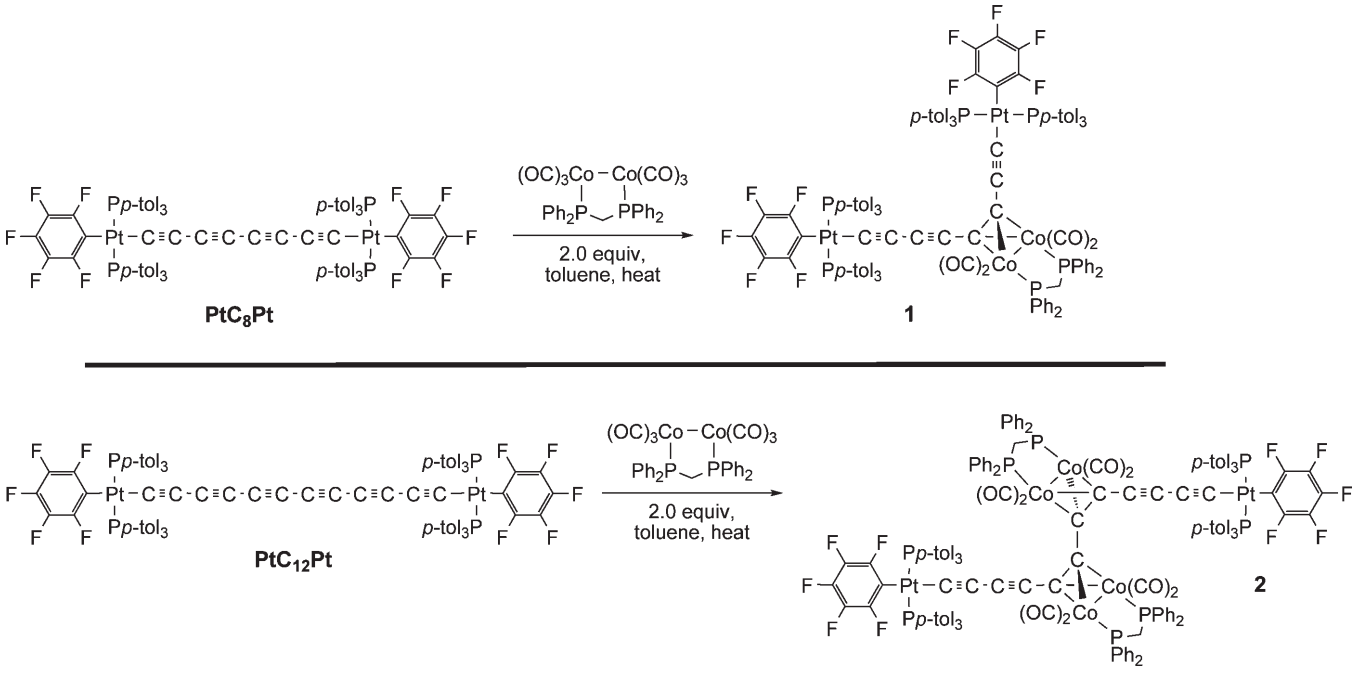

which the quantity or noncrystalline nature precludes detailed characterization.

Our research group has had a particular interest in the synthesis of dirhenium and diplatinum polyynediyl complexes.[6−8] The dirhenium complexes can be isolated with $(C{\equiv}C)_{10}$ or C_{20} chains.[6] The diplatinum complexes can be prepared with $(C{\equiv}C)_{14}$ or C_{28} chains, and their stabilities suggest that species with still longer chains should remain isolable.[8] Hence, we were interested in exploring the chemistry of a representative series of complexes with $Co_2(CO)_8$ or $Co_2(CO)_6(L)_2$ precursors. Any adducts would furthermore be of interest from the standpoint of "chain walking" of ML_n fragments, processes that so far have been observed over a more limited number of unsaturated carbon atoms.[13] Accordingly, reactions of diplatinum complexes of the formula *trans*,*trans*-$(C_6F_5)(p\text{-}tol_3P)_2Pt(C{\equiv}C)_mPt(Pp\text{-}tol_3)_2(C_6F_5)$ (**PtC$_{2m}$Pt**) were investigated, as detailed below.

Results

Following a standard protocol, a toluene solution of $Co_2(CO)_8$ and $Ph_2PCH_2PPh_2$ (1:1 mol ratio) was stirred under an inert atmosphere at 65 °C for 4 h to generate $Co_2(CO)_6(\mu\text{-}Ph_2PCH_2PPh_2)$.[14] As shown in Scheme 1 (top), a solution of the octatetrayne complex *trans*,*trans*-$(C_6F_5)(p\text{-}tol_3P)_2Pt(C{\equiv}C)_4Pt)(Pp\text{-}tol_3)_2(C_6F_5)$ (**PtC$_8$Pt**)[8] was added (0.5 equiv or 2:1 Co_2/Pt_2), and the mixture was refluxed for 2 h. A chromatographic workup (silica gel) gave **PtC$_8$Pt** (18%) and a new compound (**1**) as a deep red solid (53%). The latter was characterized by NMR (^{1}H, ^{13}C, ^{31}P), IR, and UV−visible spectroscopy, FAB mass spectrometry, and microanalysis, as summarized in the Experimental Section. When analogous reactions were conducted using a 1:1 Co_2/Pt_2 stoichiometry, conversions were lower.

The FAB mass spectrum suggested that **1** was a $Co_2(CO)_4(\mu\text{-}Ph_2PCH_2PPh_2)$ adduct of **PtC$_8$Pt**, as evidenced by an ion corresponding to a $M^+ - 2CO$ peak. Accordingly, a ^{1}H NMR spectrum (CD_2Cl_2) showed two $Ph_2PCHH'PPh_2$ signals (1:1) integrating to 2H and two $p\text{-}C_6H_4CH_3$ signals, corresponding to the $(p\text{-}tol_3P)_2PtC{\equiv}CC(Co)_2$ and $(p\text{-}tol_3P)_2PtC{\equiv}CC{\equiv}C(Co)_2$ moieties (1:1), integrating to 36H. One $Ph_2PCHH'PPh_2$ signal was resolved into a triplet of doublets, with a $^2J_{HP}$ value of 9.7 Hz and a $^2J_{HH'}$ value of 13.2 Hz. These peaks are usually reported as multiplets, but in a few other cases similar couplings have been observed ($^2J_{HP} = 10.5-10.3$ Hz, $^2J_{HH'} = 13.2-13.1$ Hz).[15] A ^{1}H NMR spectrum in $CDCl_3$ showed the isolated material to be a CH_2Cl_2 monosolvate, consistent with the microanalysis.

The ^{13}C NMR spectrum showed two $p\text{-}C_6H_4CH_3$ signals, two CO signals, and eight signals between 117.7 and 67.3 ppm. The CO resonances were broad ($w_{1/2}$ = 22−14 Hz), but as with all other complexes cited in this paper did not show any resolved phosphorus coupling. The eight signals were assigned to the C_2Co_2 and three C≡C linkages. Previous studies have established that the Co_2C_2 signals remain in the range of the C≡C signals.[15,16] Due to the two symmetry equivalent phosphorus atoms present on both endgroups and the Co_2 moiety, triplets might be expected. The downfield 117.5 ppm signal was quite broad ($w_{1/2}$ = 30 Hz), as was a 106.0 ppm signal ($w_{1/2}$ = 20 Hz). On the basis of previous studies, the former can be confidently assigned to

(13) (a) Strawser, D.; Karton, A.; Zenkina, O. V.; Iron, M. A.; Shimon, L. J. W.; Martin, J. M. L.; van der Boom, M. E. *J. Am. Chem. Soc.* **2005**, *127*, 9322. (b) Zenkina, O. V.; Karton, A.; Freeman, D.; Shimon, L. J. W.; Martin, J. M. L.; van der Boom, M. E. *Inorg. Chem.* **2008**, *47*, 5114, and references therein.

(14) Chang, Y.-C.; Lee, J.-C.; Hong, F.-E. *Organometallics* **2005**, *24*, 5686.

(15) Arnanz, A.; Marcos, M.-L.; Moreno, C.; Farrar, D. H.; Lough, A. J.; Yu, J. O.; Delgado, S.; González-Velasco, J. *J. Organomet. Chem.* **2004**, *689*, 3218. For instructive examples of couplings involving the $Ph_2PCHH'PPh_2$ ^{1}H NMR signals, see Figure 1 therein.

(16) (a) Diederich, F.; Rubin, Y.; Chapman, O. L.; Goroff, N. S. *Helv. Chim. Acta* **1994**, *77*, 1441. (b) Low, P. J.; Rousseau, R.; Lam, P.; Udachin, K. A.; Enright, G. D.; Tse, J. S.; Wayner, D. D. M.; Carty, A. J. *Organometallics* **1999**, *18*, 3885.

Table 1. Crystallographic Data for 1·$(CH_2Cl_2)_{0.5}$(THF)

empirical formula	$C_{137.50}H_{113}ClCo_2F_{10}O_5P_6Pt_2$ ($C_{133}H_{104}ClCo_2F_{10}O_4P_6Pt_2\cdot 0.5CH_2Cl_2\cdot C_4H_8O$)
fw	2764.59
temperature [K]	173(2)
wavelength [Å]	0.71073
cryst syst	triclinic
space group	$P\bar{1}$
unit cell dimensions:	
a [Å]	16.2380(3)
b [Å]	19.5179(4)
c [Å]	23.3774(4)
α [deg]	79.314(1)
β [deg]	71.186(1)
γ [deg]	82.223(1)
volume [Å^3]	6868.8(2)
Z	2
ρ_{calc} [Mg/m^3]	1.337
μ [mm^{-1}]	2.419
F(000)	2770
cryst size [mm^3]	0.20 × 0.15 × 0.10
θ range for data collection	4.21 to 26.03°
index ranges	$-20 \le h \le 20$ $-24 \le k \le 24$ $-28 \le l \le 28$
reflns collected	48 032
indep reflns	26 225 [R(int) = 0.0407]
max. and min transmn	0.7939 and 0.6433
data/restraints/params	26 225/0/1493
goodness-of-fit on F^2	1.069
final R indices [$I > 2\sigma(I)$]	R1 = 0.0588, wR2 = 0.1487
R indices (all data)	R1 = 0.0981, wR2 = 0.1901

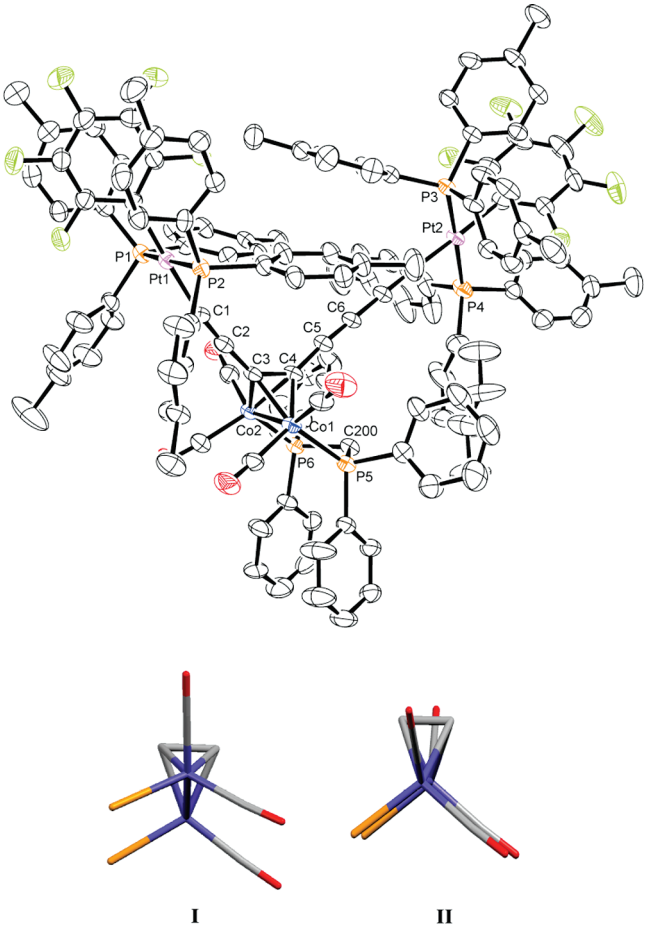

Figure 1. (Top) Thermal ellipsoid plot (30% probability level) of 1·$(CH_2Cl_2)_{0.5}$(THF) with solvate molecules omitted. (Bottom) Newman-type projections involving the pseudotetrahedral Co_2C_2 core.

one of the PtC≡ carbon atoms.[7,8] Only for one signal (81.4 ppm) was coupling resolved (J_{CP} = 17 Hz). With other $Co_2(CO)_4(\mu\text{-}Ph_2PCH_2PPh_2)$ adducts, the $^2J_{CP}$ values are either modest (e.g., J_{CP} = 9.8−4.1 Hz)[15,16] or unresolved. In any case, the ^{13}C NMR data, together with the two *p*-$C_6H_4C\underline{H}_3$ ^{1}H signals, exclude any rapid equilibrium in which the dicobalt moiety migrates from one C≡C linkage to another.

However, NMR spectra at lower temperatures evidenced other modes of dynamic behavior (below). In order to unambiguously confirm the assignment and help interpret these NMR data, the crystal structure of a mixed 0.5·CH_2Cl_2/THF solvate of **1** was determined as outlined in Table 1 and detailed in the Experimental Section. The molecular structure, which is depicted in Figure 1, showed **1** to have the composition *trans*,*trans*-$(C_6F_5)(p\text{-}tol_3P)_2PtC{\equiv}CC_2[Co_2(CO)_4(\mu\text{-}PPh_2CH_2PPh_2)](C{\equiv}C)_2Pt(P\textit{p}\text{-}tol_3)_2(C_6F_5)$, with the dicobalt moiety bound to one of the two sterically less encumbered C≡C linkages remote from the platinum atoms. Key metrical parameters are summarized in Table 2.

With regard to phenomena discussed below, note that the P−Pt−P axis of the $(p\text{-}tol_3P)_2PtC{\equiv}CC(Co)_2$ moiety (upper left, Figure 1) is essentially parallel to the cobalt−cobalt bond, and the other P−Pt−P axis, on the endgroup more distant from the cobalt atoms, is roughly perpendicular to the cobalt−cobalt bond. These relationships can be quantified by various plane/plane angles, such as those defined by P1−Pt1−P2−C3 and Co1−Co2−Pt1 or P3−Pt2−P4−C4 and Co1−Co2−Pt2, as summarized in Table 2. As expected visually, the values (5.2° and 63.1°) are reasonably close to 0° and 90°. Alternatively, the angle between the endgroup planes defined by P1−Pt1−P2−C3 and P3−Pt2−P4−C4 is 87.1°.

As is also found with crystalline **PtC$_8$Pt**[7a] and many related compounds,[17] a $C_6H_4CH_3/C_6F_5/C_6H_4CH_3$ stacking interaction is evident on each platinum endgroup. This can be quantified by the average distance between the midpoints of the rings[17] and C_{ipso}−P−Pt−C_{ipso} torsion angles that are close to zero (Table 2). The endgroup with the torsion angles closer to zero (Pt1, 0.2° and −3.0° vs Pt2, 12.3° and 24.7°) exhibits the shorter average midpoint distance (3.57 Å vs 3.85 Å).

The structure of **1** clearly renders the PC$\underline{HH}$'P protons diastereotopic and the platinum endgroups inequivalent, consistent with the two sets of ^{1}H NMR signals noted above. As shown in Figure 2, a ^{31}P NMR spectrum in CD_2Cl_2 at 10 °C showed a sharp singlet with two ^{195}Pt satellites (δ 16.8 ppm, $^1J_{PtP}$ = 2658 Hz) and a broad singlet without obvious satellites (δ 38.6 ppm). These were assigned to the *p*-$tol_3\underline{P}$ and $Co\underline{P}Ph_2$ signals, respectively. However, since the

(17) (a) Stahl, J.; Mohr, W.; de Quadras, L.; Peters, T. B.; Bohling, J. C.; Martín-Alvarez, J. M.; Owen, G. R.; Hampel, F.; Gladysz, J. A. *J. Am. Chem. Soc.* **2007**, *129*, 8282. (b) de Quadras, L.; Bauer, E. B.; Mohr, W.; Bohling, J. C.; Peters, T. B.; Martín-Alvarez, J. M.; Hampel, F.; Gladysz, J. A. *J. Am. Chem. Soc.* **2007**, *129*, 8296. (c) de Quadras, L.; Bauer, E. B.; Stahl, J.; Zhuravlev, F.; Hampel, F.; Gladysz, J. A. *New J. Chem.* **2007**, *31*, 1594. (d) Owen, G. R.; Stahl, J.; Hampel, F.; Gladysz, J. A. *Chem.—Eur. J.* **2008**, *14*, 73.

Table 2. Key Interatomic Distances [Å] and Bond and Other Angles [deg] for 1·$(CH_2Cl_2)_{0.5}$(THF)

Pt1−C1	1.987(8)
C1−C2	1.203(12)
C2−C3	1.401(12)
C3−C4	1.387(11)
C4−C5	1.376(11)
C5−C6	1.220(11)
C6−C7	1.376(11)
C7−C8	1.205(12)
C8−Pt2	2.001(9)
Pt1−P1	2.310(2)
Pt1−P2	2.308(2)
Pt2−P3	2.302(2)
Pt2−P4	2.293(3)
Co1−C3	1.967(9)
Co1−C4	1.957(8)
Co2−C3	1.954(8)
Co2−C4	1.970(8)
Co1−P5	2.229(3)
Co2−P6	2.219(2)
Pt1−Pt2	10.298
sum, bond lengths Pt1−Pt2	13.155
average π stacking, Pt1[a]	3.57
average π stacking, Pt2[a]	3.85
C2−C1−Pt1	171.3(7)
C7−C8−Pt2	177.4(8)
C4−C3−C2	139.2(7)
C5−C4−C3	138.7(8)
C4−C3−Co1	68.9(5)
C4−C3−Co2	69.9(5)
C3−C4−Co1	69.7(5)
C3−C4−Co2	68.7(5)
C4−Co1−Co2	51.0(2)
C3−Co1−Co2	50.5(2)
P5−C200−P6	109.0(4)
C200−P5−Co1	108.8(3)
C200−P6−Co2	109.2(3)
P5−Co1−Co2	96.43(7)
P6−Co2−Co1	96.73(8)
C201−Co2−Co1	100.9(4)
C204−Co1−Co2	100.2(4)
C202−Co2−Co1	148.2(3)
C203−Co1−Co2	147.6(3)
P5−Co1−Co2−P6	−0.86(9)
C204−Co1−Co2−C201	0.8(5)
C203−Co1−Co2−C202	2.3(9)
C3−Co1−Co2−C4	54.3(4)
C21[b]−P1−Pt1−C11[b]	0.2(4)
C11[b]−Pt1−P2−C71[b]	−3.0(4)
C121[b]−P3−Pt2−C111[b]	12.3(4)
C111[b]−Pt2−P4−C161[b]	24.7(5)
P1−Pt1−P2−C3 and Co1−Co2−Pt1[c]	5.2
P3−Pt2−P2−C4 and Co1−Co2−Pt2[c]	63.1
P1−Pt1−P2−C3 and P3−Pt2−P4−C4[c]	87.1

[a] Average distance between midpoints of the C_6F_5 and C_6H_5 rings. [b] An ipso phenyl carbon. [c] Angles between (least-squares) planes defined by the indicated atoms.

two endgroups were noted to give different *p*-$C_6H_4\underline{CH_3}$ signals above, the *p*-$tol_3\underline{P}$ signals are presumed to be accidentally degenerate. Additional low-temperature ^{31}P and ^{1}H NMR spectra were subsequently recorded (Figures 2 and 3), and these data are interpreted in the Discussion section.

As shown in Scheme 1 (bottom), an analogous reaction was conducted with $Co_2(CO)_6(\mu\text{-}Ph_2PCH_2PPh_2)$ and **PtC$_{12}$Pt**, again employing a 2:1 Co_2/Pt_2 stoichiometry. Silica gel thin-layer chromatography indicated the presence of several products. However, partial decomposition was

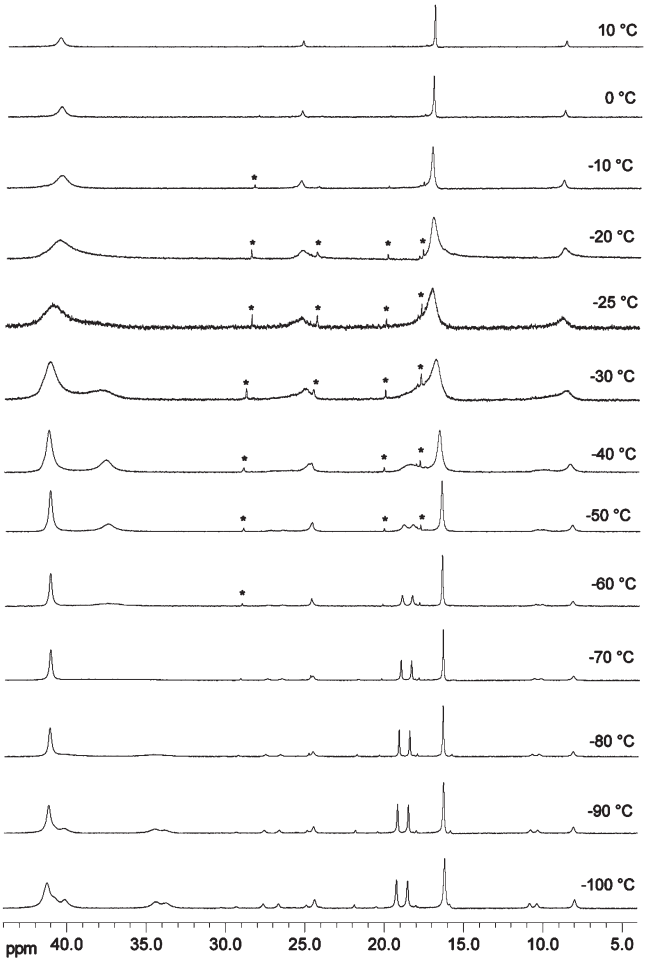

Figure 2. Variable-temperature $^{31}P\{^{1}H\}$ NMR spectra (10 to −100 °C) of **1** in CD_2Cl_2. The peaks marked * indicate impurities visible in spectra with extensively broadened peaks.

evident as the plate developed. Using preparative silica gel columns, it only proved possible to isolate one of the major products, **2** (12%). The mass spectrum showed a molecular ion consistent with the 2:1 adduct *trans*, *trans*-$(C_6F_5)(p\text{-}tol_3P)_2Pt(C{\equiv}C)_2C_2[Co_2(CO)_4(\mu\text{-}PPh_2CH_2PPh_2)]C_2[Co_2(CO)_4(\mu\text{-}PPh_2CH_2PPh_2)](C{\equiv}C)_2Pt(P\textit{p}\text{-}tol_3)_2(C_6F_5)$. The ^{13}C NMR spectrum exhibited only six C≡C and Co_2C_2 signals, the furthest downfield of which (106.5, 104.2 ppm) were broad ($w_{1/2}$ = 33−25 Hz) and none of which exhibited resolved coupling to phosphorus. The ^{1}H and ^{13}C NMR spectra showed only a single set of *p*-$C_6H_4\underline{CH_3}$ signals and the ^{31}P NMR spectrum only a single set of *p*-$tol_3\underline{P}$ signals.

The preceding data suggest a symmetrical structure, the most logical of which would have the dicobalt moieties bound to C≡C bonds remote from the endgroups. Bruce has reported a related bis-$Co_2(CO)_4(\mu\text{-}Ph_2PCH_2PPh_2)$ adduct derived from a complex with a $W(C{\equiv}C)_4W$ backbone.[11a] Hence, the structure depicted in Scheme 1 is proposed. When ^{31}P NMR spectra of **2** were recorded in CD_2Cl_2 at low temperature, the signals shifted somewhat and became noticeably broadened at −80 °C (36.7 and 16.7 ppm). Very near the freezing point (−100 to −110 °C), the Co*P* signals broadened dramatically, and two *p*-$tol_3\underline{P}$ signals became apparent. However, ^{1}H NMR spectra showed only a gradual broadening of the PC$\underline{HH'}$P signals as the sample was cooled to −80 °C.

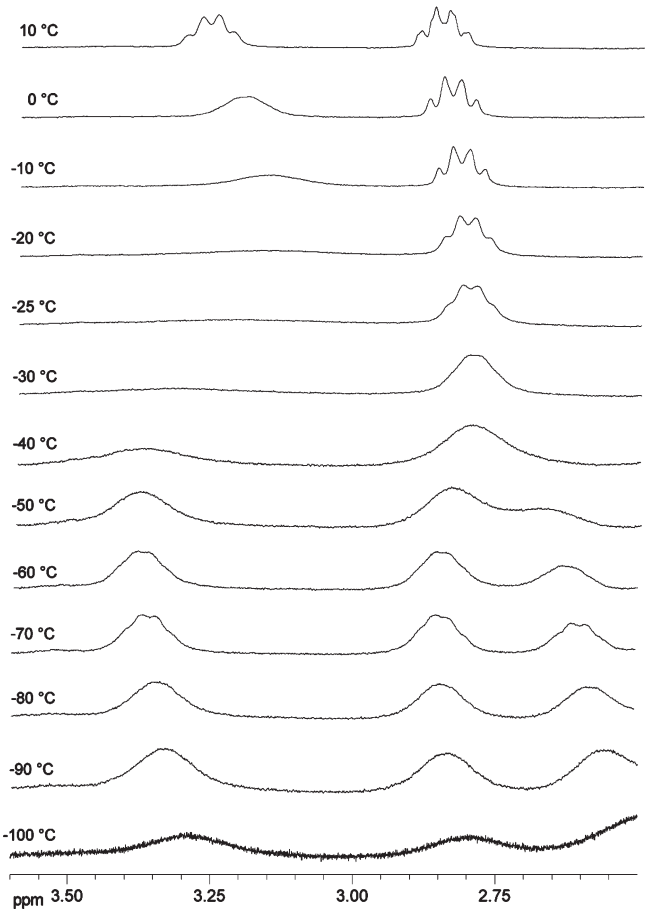

Figure 3. Variable-temperature ^{1}H NMR spectra (10 to −100 °C) of **1** in CD_2Cl_2. The upfield cutoff of the spectra is selected to remove intense and markedly broadened $C_6H_4C\underline{H}_3$ signals.

An analogous reaction was conducted with $Co_2(CO)_6(\mu$-$Ph_2PCH_2PPh_2)$ and **PtC$_{16}$Pt**. Unfortunately, the products appeared to be even more sensitive to silica gel, as partial decomposition was obvious with every column. Nonetheless, a small quantity of a 2:1 adduct (**3**) could be isolated, as evidenced by mass spectrometry. However, the sample was not homogeneous by ^{31}P NMR, suggesting a mixture of isomers differing in the dicobalt positions.

Complexes **1** and **2** were compared in additional ways. As expected, the UV−visible spectra showed more intense and red-shifted maxima for the longer chained species **2** (nm (ε, M^{-1} cm^{-1}), CH_2Cl_2: 317 (17 900), 334 (18 300), 359 (17 200) vs 326 (8800), 349 (8200)). However, the parent complexes **PtC$_{2m}$Pt** exhibited much more intense absorptions (e.g., 315 (ε 101 000), 336 (ε 267 000), and 359 (ε 432 000) nm for **PtC$_{12}$Pt**).[7a]

Cyclic voltammograms were run under conditions previously used for the parent complexes (1.25×10^{-5} M, n-$Bu_4N^+BF_4^-/CH_2Cl_2$ at 22.5 ± 2 °C; Pt working and counter electrodes, potential vs Ag wire pseudoreference; scan rate 100 mV s^{-1}; ferrocene = 0.46 V).[7,8] Both **1** and **2** exhibited two irreversible oxidations ($E_{p,a}$ = **1**, 0.58 and 1.37 V; **2**, 0.56 and 0.86 V), as compared to a single partially reversible oxidation for **PtC$_8$Pt** and **PtC$_{12}$Pt** ($E_{p,a}$ [V]/$E_{p,c}$ [V]/$E°$ [V]/$i_{c/a}$ = 1.26/1.14/1.20/0.48 and 1.47/1.31/1.39/low). The potentials show that the cobalt-containing complexes are more easily oxidized and are close to those of other $Co_2(CO)_4(L)_2$/alkyne adducts that have been measured in CH_2Cl_2.[18] Both **1** and **2** also exhibited irreversible reductions ($E_{p,c}$ = **1**, −0.84 V; **2**, −0.86 V), in contrast to **PtC$_8$Pt** and **PtC$_{12}$Pt**, which exhibit no reductions prior to the solvent-induced limit (ca. −1.3 V). As expected from previous studies,[18] this must reflect chemistry associated with the Co_2C_2 core.

(18) (a) Duffy, N. W.; McAdam, C. J.; Robinson, B. H.; Simpson, J. *J. Organomet. Chem.* **1998**, *565*, 19, and references therein. (b) Medina, R. M.; Moreno, C.; Marcos, M. L.; Castro, J. A.; Benito, F.; Arnanz, A.; Delgado, S.; Gonzalez-Velasco, J.; Macazaga, M. J. *Inorg. Chim. Acta* **2004**, *357*, 2069.

Discussion

1. Synthesis and Structure. Scheme 1 and other data show that the $Co_2(CO)_4(\mu$-$Ph_2PCH_2PPh_2)$ fragment readily binds to the sp carbon chain of diplatinum polyynediyl complexes **PtC$_{2m}$Pt** for which $2m \geq 8$. Complex **3** features what is to our knowledge the longest polyyne coordinated by any type of $Co_2(CO)_4(L)_2$ fragment to date, with **2** representing the record for a fully characterized species. However, the PtC≡C linkages do not appear to be accessible, presumably due to steric grounds. Many $Co_2(CO)_6$ derivatives of polyynediyl complexes have been reported, but preliminary efforts with our diplatinum building blocks were less promising and handicapped by the loss of the diagnostic NMR signals associated with the diphosphine ligand $Ph_2PCH_2PPh_2$.

Bruce has reported that a very similar reaction of $Co_2(CO)_6(\mu$-$Ph_2PCH_2PPh_2)$ and the diruthenium octatetraynediyl complex $(\eta^5$-$C_5H_5)(CO)_2Ru(C{\equiv}C)_4Ru(CO)_2(\eta^5$-$C_5H_5)$ (2.2:1.0 Co_2/Ru_2 ratio, refluxing benzene) affords an adduct analogous to **1** in 56% yield after chromatography. Bruce has also reported several $Co_2(CO)_4(\mu$-$Ph_2PCH_2PPh_2)$ derivatives of the ditungsten octatetraynediyl complex $(\eta^5$-$C_5H_5)(CO)_3W(C{\equiv}C)_4W(CO)_3(\eta^5$-$C_5H_5)$. These include a 1:1 adduct involving the WC≡C linkage and a 2:1 adduct derived from the two WC≡C$\underline{C}$≡$\underline{C}$ linkages.[11a] However, we are unaware of any complexes involving $L_nMC{\equiv}C$ linkages where the ligand set L_n includes a bulky triaryl phosphine. Bruce's 2:1 adduct can be viewed as a lower homologue of **2**, which similarly involves dicobalt binding to adjacent C≡C linkages.

Upon complexation of **PtC$_8$Pt**, the Pt−Pt distance decreases from 12.895(3) Å[7a] to 10.298 Å in **1**. At the same time, the sum of the intervening bond lengths increases from 12.905 Å[7a] to 13.155 Å. The bond lengths and angles associated with the pseudotetrahedral Co_2C_2 core are close to those reported by Bruce and others previously. As illustrated by **I** in Figure 1 (bottom) and found in the other molecules above, the $Co(CO)_2P$ moieties adopt roughly staggered conformations with respect to the other three atoms (CoC_2) that comprise the tetrahedron. This in turn leads to syn relationships between the Co−CO and Co−P bonds on opposite cobalt atoms, as depicted in **II** (Figure 1) and reflected by the near-zero C−Co−Co−C and P−Co−Co−P torsion angles (−0.86(9)° to 2.3(9)°, Table 2). The Co−Co−CO bond angles associated with one pair of CO ligands (100.9(4)° and 100.2(4)°) and the Co−Co−P bond angles (96.43(7)° and 96.73(8)°) are close to 90°. In contrast, the Co−Co−CO bond angles associated with the other pair of CO ligands are much larger (148.2(3)° and 147.6(3)°). Similar patterns are observed with related complexes and are in accord with a bonding model involving dsp^3-hybridized or trigonal-bipyramidal cobalt in which the larger bond angles reflect pseudoaxial ligands and the smaller angles pseudoequatorial.[10]

Figure 1 also shows that the P−Co−Co−P linkage can be viewed as roughly anti to the C−C≡CPt moiety, and one (pseudoequatorial) OC−Co−Co−CO linkage can be viewed as roughly anti to the C−C≡CC≡CPt moiety. Hypothetical structures in which these relationships are reversed will be considered below. In the complexes structurally characterized by Bruce,[11] the P−Co−Co−P linkages adopt conformations that place them roughly anti to a variety of moieties (e.g., ML_n endgroups, $Co_2C-C Co_2$ linkages). There appears to be no intrinsic electronic preference.

Although the cyclic voltammetry data establish that **1** and **2** do not undergo any well-defined oxidations or reductions, metal polyynediyl complexes often exhibit a rich redox chemistry.[6,19] However, only a few other types of well-defined reactions involving polyynediyl ligands have been reported. These include cycloaddition/ring-opening sequences employing TCNE,[11b,20] insertions of isonitriles[21] or iron and ruthenium carbonyl fragments,[11b,22] and simple protonations.[23] There have also been hints of oxidative carbon−carbon bond forming reactions[24] and good leads for C≡C metathesis reactions.[25] In all cases, an ongoing challenge, especially at longer chain lengths, will be selectivity with respect to the C≡C linkage derivatized, as exemplified in the above dicobalt chemistry.

2. Dynamic Behavior. Most previous studies of dynamic behavior of $Co_2(CO)_4(\mu\text{-}Ph_2PCH_2PPh_2)$ adducts have involved symmetrical alkynes.[14,26] In the higher temperature rapid exchange limit, a single ^{1}H NMR signal is usually observed for the methylene protons of the bridging $Ph_2PCH_2PPh_2$ ligand (H_a, H_b). At the lower temperature slow exchange limit, two signals are found. This has been interpreted in terms of the equilibrium **IIIa** ⇌ **Va** shown in Scheme 2, which involves a rotation of the ligands about the Co−Co axis and additional structural nuances (e.g., interconversion of pseudoaxial and pseudoequatorial CO ligands). This exchanges the positions of H_b (syn to the alkyne ligand in **IIIa**) and H_a (syn to the alkyne ligand in **Va**). In principle, two sets of signals for the alkyne substituents and CO ligands should also be observable at the slow exchange limit.

Importantly, this situation changes when the alkyne is not symmetrically substituted. In such cases, the species in Scheme 2, **IIIb** and **Vb**, are no longer identical. They are diastereomers and one should predominate (e.g., that in which the bulkier R/R′ group is anti to the diphosphine).

Scheme 2. Conformational Equilibria in $Co_2(CO)_4(\eta^2\text{-}Ph_2PCH_2PPh_2)$ Adducts of Symmetrical and Unsymmetrical Alkynes

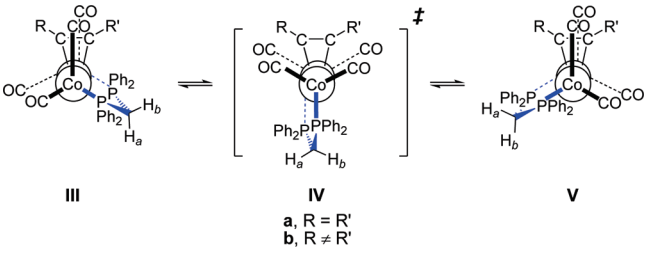

At the slow exchange limit, there should be two unequal sets of two equal H_a/H_b signals. At the rapid exchange limit, there should be one set of two equal H_a/H_b signals. For similar reasons, the diphosphine ligand should give two unequal ^{31}P NMR signals at the slow exchange limit.

We are aware of only a few such complexes where NMR data of any type have been recorded below room temperature.[14,26b] In the case of an alkyne with R/R′ = Ph/P(*t*-Bu)$_2$, ^{1}H NMR data have been reported only at room temperature, but ^{31}P NMR spectra (20 to −90 °C) show the decoalescence of the diphosphine singlet into two doublets with similar areas and coupling constants, with the P(*t*-Bu)$_2$ signal remaining a singlet. This coupling would appear to require additional equilibria involving species of lower symmetry than those in Scheme 2. The authors concluded that the data were "in good agreement with the low symmetry of the compound revealed in the solid state".[14]

The preceding results provide a starting point for analyzing the variable-temperature ^{31}P and ^{1}H NMR spectra in Figures 2 and 3. As shown in Figure 3, the two equal H_a/H_b signals broaden at unequal rates (downfield faster), as is easily rationalized if the chemical shift difference for H_a in the limiting structures **IIIb** and **Vb** (Scheme 2) differs significantly from that for H_b. At −60 °C, three signals are present at δ 3.37, 2.85, and 2.63 in an area ratio of 33:36:31 (−70 °C, 28:34:38). Further interpretation is complicated by the nearby $C_6H_4C\underline{H}_3$ signal (δ 2.29), which markedly broadens at lower temperatures and possibly obscures a relevant peak. No other decoalescence phenomena are noted in spectra recorded down to −100 °C. In any case, these observations are easily rationalized within the framework of the equilibrium **IIIb**/**Vb** in Scheme 2, which is recast in Scheme 3 (top) as **IIIc**/**Vc**.

As shown in Figure 2, when ^{31}P NMR spectra are recorded at lower temperatures, the diphosphine signal (40.7 ppm, 10 °C) decoalesces into two broad singlets of unequal areas (41.2 and 37.6 ppm, −40 °C; 67:33). We interpret this as reflecting a ca. 2:1 **Vc**/**IIIc** mixture, in which the diphosphine ligand of the major isomer is closer (syn) to the endgroup with the longer sp chain, per the crystal structure. In this case, the area ratios for the H_a/H_b ^{1}H signals given above would require that those of the minor isomer overlap. For the minor isomer, further decoalescence of ^{31}P NMR signals occurs, affording what appears to be two doublets with similar areas and coupling constants (−100 °C). One signal is partially obscured by the nearby 41.2 ppm peak, complicating analysis (d, 34.1 ppm, J = 100.0 Hz for the unobscured signal or dd, 33.3 ppm, J = 1034.9, 103.5 Hz via fitting routines). This parallels the behavior of the Ph/P(*t*-Bu)$_2$ system mentioned

(19) Paul, F.; Lapinte, C. In *Unusual Structures and Physical Properties in Organometallic Chemistry*; Gielen, M.; Willem, R.; Wrackmeyer, B., Eds.; Wiley: New York, 2002; pp 220−291.
(20) (a) Bruce, M. I.; Hall, B. C.; Kelley, B. D.; Low, P. J.; Skelton, B. W.; White, A. H. *J. Chem. Soc., Dalton Trans.* **1999**, 3719. (b) Onitsuka, K.; Ose, N.; Ozawa, F.; Takahashi, S. *J. Organomet. Chem.* **1999**, *578*, 169.
(21) Takei, F.; Hayashi, H.; Onitsuka, K.; Kobayashi, N.; Takahashi, S. *Angew. Chem., Int. Ed.* **2001**, *40*, 4092. *Angew. Chem.* **2001**, *113*, 4216.
(22) (a) Akita, M.; Koike, T. *Dalton Trans.* **2008**, 3523, and references therein. (b) Bruce, M. I.; Ellis, B. G.; Skelton, B. W.; White, A. H. *J. Organomet. Chem.* **2000**, *607*, 137. (c) Byrne, L. T.; Hos, J. P.; Koutsantonis, G. A.; Skelton, B. W.; White, A. H. *J. Organomet. Chem.* **2000**, *598*, 28.
(23) Coat, F.; Guillemot, M.; Paul, F.; Lapinte, C. *J. Organomet. Chem.* **1999**, *578*, 76.
(24) Owen, G. R.; Hampel, F.; Gladysz, J. A. *Organometallics* **2004**, *23*, 5893.
(25) Dembinski, R.; Szafert, S.; Haquette, P.; Lis, T.; Gladysz, J. A. *Organometallics* **1999**, *18*, 5438.
(26) (a) Hong, F.-E.; Chang, Y.-C.; Chang, R.-E.; Chen, S.-C.; Ko, B.-T. *Organometallics* **2002**, *21*, 961. (b) Hong, F.-E.; Lai, Y.-C.; Ho, Y.-J.; Chang, Y.-C. *J. Organomet. Chem.* **2003**, *688*, 161. (c) Hong, F.-E.; Chang, Y.-C.; Chang, C.-P.; Huang, Y.-L. *Dalton Trans.* **2004**, 157.

Scheme 3. Selected Conformational Equilibria of 1

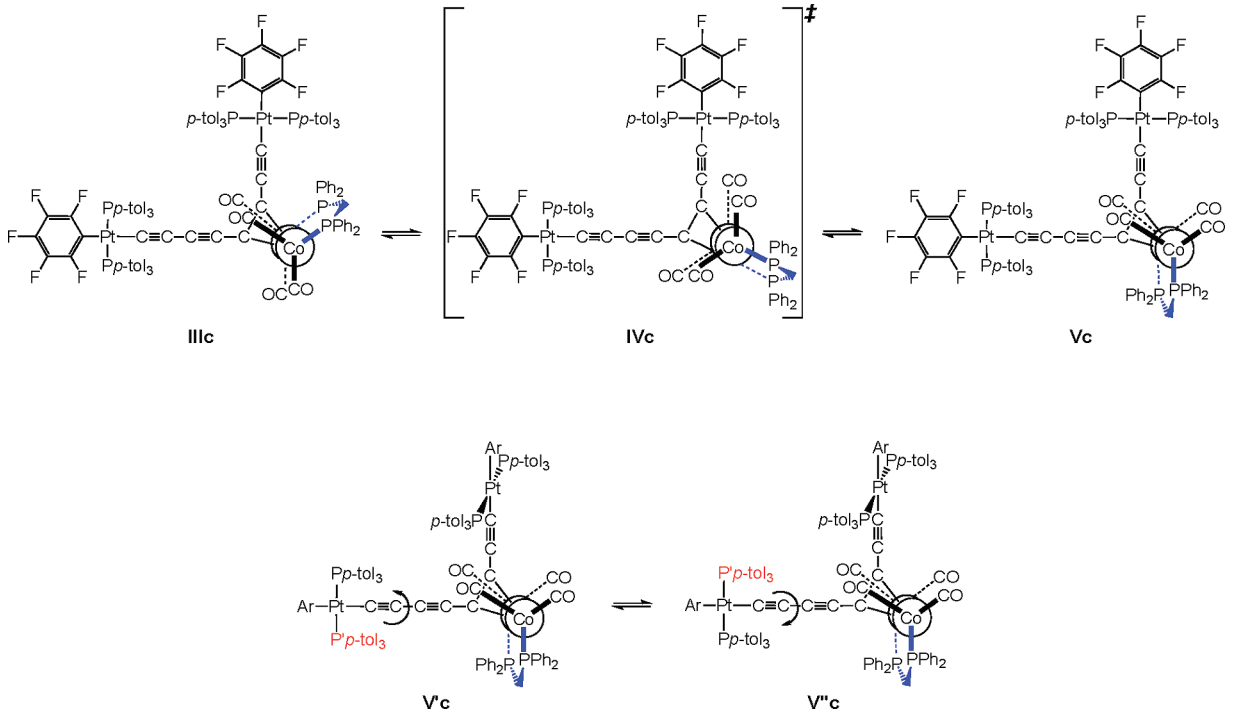

above[14] and requires equilibria involving species of lower symmetries than those in Schemes 2 and 3.[27]

In view of the distinct $C_6H_4\underline{CH_3}$ ^{1}H and ^{13}C NMR signals found for the *p*-tol$_3$P ligands on opposite platinum termini in **1**, two ^{31}P signals would similarly be expected. Hence, we assume that the single signal observed at ambient probe temperature or 10 °C (Figure 2) reflects an accidental degeneracy. In any event, upon further cooling, this signal decoalesces into three signals with a 2:1:1 area ratio (52:24:24, −100 °C). The two less intense signals are provisionally assigned to the (*p*-tol$_3$P)$_2$PtC≡CC≡C(Co)$_2$ endgroup, which as shown in Figure 1 features a P−Pt−P axis that is perpendicular to the Co−Co bond. This results in *p*-tol$_3$P ligands that have "cis" and "trans" relationships to the P−Co−Co−P linkage, as highlighted in **V′c** and **V″c** in Scheme 3 (bottom). Exchange of the two phosphine ligands by rotation about the Pt−C≡C−C≡C−C linkage must be rapid on the NMR time scale at room temperature.[28]

Although all of the *p*-tol$_3$P signals in Figure 2 can be accounted for, these data do not themselves demand an equilibrium between the limiting structures **IIIc** and **Vc**. However, this is required by the low-temperature behavior of the diphosphine ^{31}P NMR signals in Figure 2 and the PCH$_2$P ^{1}H NMR signals in Figure 3. Hence, we presume that additional decoalescence phenomena involving the *p*-tol$_3$P ligands would be observed at still lower temperatures. In any event, the principle modes of dynamic behavior of **1** have been defined, and additional nuances may be elucidated through further studies.

3. Conclusions. This study has established the ready availability of Co$_2$(CO)$_4$(*μ*-Ph$_2$PCH$_2$PPh$_2$) adducts of diplatinum polyynediyl complexes **PtC$_{2m}$Pt** with $2m \geq 8$. However, the low yield and many byproducts that accompany the incompletely characterized hexadecaoctaynediyl-derived complex **3** portend increasing selectivity and polyderivatization problems at longer chain lengths. This in turn suggests that it will be challenging to develop any well-defined ligand-based chemistry of polyynediyl systems with C_{20}−C_{28} bridges, apart from $L_n\underline{M-C}\equiv$ insertion reactions.

Nonetheless, the octatetraynediyl-derived complex **1** can be prepared in good yield and exhibits a fascinating range of dynamic properties. These include (1) previously documented processes, such as the exchange of CO and diphosphine positions as sketched in Scheme 2, (2) new phenomena, such as restricted rotation about −(C≡C)$_n$− endgroup axes as illustrated in Scheme 3 (bottom), and (3) processes that remain to be fully delineated, per the diphosphine signals at the lowest temperatures in Figure 2. Additional aspects of the chemistry of polyynediyl complexes **PtC$_{2m}$Pt** will be detailed in future publications.

Experimental Section

General Data. Reactions were conducted under dry nitrogen atmospheres using standard Schlenk techniques, but workups were carried out in air. Chemicals were treated as follows: toluene, distilled from Na/benzophenone; hexanes, pentane, CH_2Cl_2, ethyl acetate, and ethanol, distilled by rotary evaporation; Co$_2$(CO)$_8$ (Acros, 95%), Ph$_2$PCH$_2$PPh$_2$ (Acros, 98%), and silica gel 60 M (Macherey-Nagel), used as received.

NMR spectra were obtained on a Bruker 400 MHz spectrometer and referenced as follows: ^{1}H NMR, residual $CHCl_3$ (δ 7.24 ppm) or $CDHCl_2$ (δ 5.32 ppm); ^{13}C NMR, internal $CDCl_3$ (77.0 ppm) or CD_2Cl_2 (53.5 ppm); ^{31}P NMR, internal H_3PO_4

(27) A reviewer has suggested that the ground state conformation of the Ph$_2$PCH$_2$PPh$_2$ ligand may be twisted, such that there is no longer an idealized mirror plane containing the CH$_2$ group and bisecting the cobalt−cobalt bond. This would rationalize the apparent dd observed in the ^{31}P NMR spectrum at −100 °C. The reviewer also raises the possibility of highly temperature dependent equilibria.

(28) In principle, a structure with opposite conformations of the platinum endgroups could also be considered. However, any structure in which the two P−Pt−P axes were parallel would lead to significant steric interactions between the endgroups. The transition state for the exchange of the *p*-tol$_3$P ligands may feature parallel axes.

capillary (δ 0.00 ppm). IR and UV−visible spectra were recorded on ASI ReactIR-1000 and Analytik Jena Specord S600 spectrometers. Mass spectra and microanalyses were obtained using Micromass Zabspec and Carlo Erba EA1110 instruments. Cyclic voltammograms were recorded as described previously.[8b]

***trans*,*trans*-$(C_6F_5)(p\text{-}tol_3P)_2PtC{\equiv}CC_2[Co_2(CO)_4(\mu\text{-}PPh_2CH_2PPh_2)](C{\equiv}C)_2Pt(Pp\text{-}tol_3)_2(C_6F_5)$ (1).** A Schlenk flask was charged with $Co_2(CO)_8$ (0.032 g, 0.098 mmol), $Ph_2PCH_2PPh_2$ (0.036 g, 0.098 mmol), and toluene (4 mL) and fitted with a condenser. The solution was stirred at 65 °C for 4 h. Then a solution of *trans*,*trans*-$(C_6F_5)(p\text{-}tol_3P)_2Pt(C{\equiv}C)_4Pt(Pp\text{-}tol_3)_2(C_6F_5)$ (**PtC$_8$Pt**;[8] 0.101 g, 0.049 mmol) in toluene (2 mL) was added. The mixture was refluxed with stirring for 2 h and allowed to cool to room temperature. The solvent was removed by rotary evaporation. The deep red residue was chromatographed on a silica gel column (35 × 2.5 cm, 30:70 v/v CH_2Cl_2/pentane). Two fractions were collected, and the solvent was removed from each by rotary evaporation and oil pump vacuum. The first gave **PtC$_8$Pt** (0.038 g, 0.018 mmol, 18%), and the second gave the monosolvate **1**·CH_2Cl_2 as a deep red solid (0.138 g, 0.052 mmol, 53%), mp (capillary) 165 °C (first appearance of liquid) to 190 °C (complete liquefaction; reproducible with resolidified sample). Anal. Calcd for $C_{133}H_{106}Co_2F_{10}O_4P_6Pt_2\cdot CH_2Cl_2$: C, 58.72; H, 4.12. Found: C, 58.83; H, 4.27.

NMR (δ, CD_2Cl_2): ^{1}H 7.57−7.42 (m, 24H, *o* to PtP), 7.12−6.85 (m, 44H, *m* to PtP, 4CoPPh), 3.02 (apparent dd, J = 23.4 Hz, 10.9 Hz, 1H, PC*H*H′P),[29] 2.50 (dt, $^2J_{HH}$ = 9.9 Hz, $^2J_{HP}$ = 12.8 Hz, 1H, PCH*H*′P),[29] 2.24 (s, 18H, CH_3), 2.20 (s, 18H, CH_3); $^{13}C\{^1H\}$[30] 206.8 (br s or m, $w_{1/2}$ = 22.1 Hz, CO), 200.9 (br s or m, $w_{1/2}$ = 20.1 Hz, CO), 141.1 (s, *p* to PtP), 140.6 (s, *p* to PtP′), 139.7 (virtual t, $^1J_{CP}$ = 23.5 Hz,[31] *i* to CoP),[29] 134.8 (virtual t, $^2J_{CP}$ = 6.3 Hz,[31] *o* to PtP), 134.6 (virtual t, $^2J_{CP}$ = 6.3 Hz,[31] *o* to PtP′), 133.3 (virtual t, $^2J_{CP}$ = 6.4 Hz,[31] *o* to CoP),[29] 130.0 (s, *p* to CoP),[29] 129.0 (virtual t, $^3J_{CP}$ = 5.5 Hz,[31] *m* to PtP), 128.8 (virtual t, $^3J_{CP}$ = 5.5 Hz,[31] *m* to PtP′), 128.4 (virtual t, $^3J_{CP}$ = 5.5 Hz,[31] *m* to CoP),[29] 128.0 (virtual t, $^1J_{CP}$ = 30.4 Hz,[31] *i* to PtP), 127.9 (virtual t, $^1J_{CP}$ = 30.4 Hz, *i* to PtP′), C≡C and Co_2C_2 at 117.7 (br s, $w_{1/2}$ = 20.1 Hz), 115.1 (s), 106.0 (br s, $w_{1/2}$ = 30.2 Hz), 98.9 (s), 88.4 (s), 81.4 (t, J_{PC} = 17.3 Hz), 73.8 (s), 67.3 (s); 30.1 (s, PC*H*$_2$P), 21.5 (s, $C_6H_4CH_3$), 21.4 (s, C′$_6$H$_4$C′H$_3$); $^{31}P\{^1H\}$ 17.0 (s, $^1J_{PtP}$ = 2672 Hz,[32] PtP), 38.3 (br s, CoP).[29]

NMR (δ, $CDCl_3$): ^{1}H 7.86−7.82 (m, 24H, *o* to PtP), 7.55−7.37 (m, 44H, *m* to PtP, 4CoPPh), 5.32 (s, 2H, CH_2Cl_2), 3.58 (apparent dd, J = 23.3 Hz, 10.2 Hz, 1H, PC*H*H′P),[29] 3.15 (dt, $^2J_{HH}$ = 13.2 Hz, $^2J_{HP}$ = 9.7 Hz, 1H, PCH*H*′P),[29] 2.61 (s, 18H, CH_3); $^{31}P\{^1H\}$ 17.1 (s, $^1J_{PtP}$ = 2693 Hz,[32] PtP), 41.0 (br s, CoP).[29]

IR (cm^{-1}, powder film): 2150/2077 (w/w, $\nu_{C\equiv C}$), 2019/1988/1961 (s/s/s, ν_{CO}). UV−vis (nm (ε, M^{-1} cm^{-1}), 1.25 × 10^{-5} M in CH_2Cl_2): 326 (8800), 349 (8200). MS:[33] 2594 (M$^+$ − 2CO, 10%), 2536 (M$^+$ − 4CO, 15%), 2234 (M$^+$ − 3CO − C_6F_5, 18%), 2154 (M$^+$ − CO − P*p*-tol$_3$ − C_6F_5, 12%), 1929 (M$^+$ − 3CO − P*p*-tol$_3$ − 2C_6F_5, 12%), 802 (Pt(P*p*-tol$_3$)$_2$]$^+$, 100%).

***trans*,*trans*-$(C_6F_5)(p\text{-}tol_3P)_2Pt(C{\equiv}C)_2C_2[Co_2(CO)_4(\mu\text{-}PPh_2CH_2PPh_2)]C_2[Co_2(CO)_4(\mu\text{-}PPh_2CH_2PPh_2)](C{\equiv}C)_2Pt(Pp\text{-}tol_3)_2(C_6F_5)$ (2).** A Schlenk flask was charged with $Co_2(CO)_8$ (0.045 g, 0.131 mmol), $Ph_2PCH_2PPh_2$ (0.050 g, 0.131 mmol), and toluene (5 mL) and fitted with a condenser. The solution was stirred at 65 °C for 2 h. Then a solution of *trans*,*trans*-$(C_6F_5)(p\text{-}tol_3P)_2Pt(C{\equiv}C)_6Pt(Pp\text{-}tol_3)_2(C_6F_5)$ (**PtC$_{12}$Pt**;[8] 0.139 g, 0.065 mmol) in toluene (2 mL) was added. The mixture was refluxed with stirring for 3 h and allowed to cool to room temperature. The solvent was removed by rotary evaporation. The deep red residue was chromatographed on a silica gel column (45 × 3 cm, 30:70 v/v CH_2Cl_2/pentane). The solvent was removed from a product-containing fraction by rotary evaporation and oil pump vacuum to give **2** as a deep red solid (0.026 g, 0.078 mmol, 12%), mp (capillary) 195 °C (first appearance of liquid) to 220 °C (complete liquefaction; reproducible with resolidified sample). Anal. Calcd for $C_{166}H_{136}Co_4F_{10}O_8P_8Pt_2\cdot CH_2Cl_2$: C, 58.86; H, 4.08. Found: C, 58.47; H, 4.14.

NMR (δ, $CDCl_3$): ^{1}H 7.65−7.34 (m, 24H, *o* to PtP), 7.21−6.88 (m, 44H, *m* to PtP, 4CoPPh), 3.39−3.22 (m, 2H, PC*H*H′P), 2.79−2.62 (m, 2H, PCH*H*′P), 2.17 (s, 36H, CH_3); $^{13}C\{^1H\}$[34] 206.7 (br s or m, $w_{1/2}$ = 20.8 Hz, CO), 200.1 (br s or m, $w_{1/2}$ = 13.9 Hz, CO), 140.3 (s, *p* to PtP), 134.3 (virtual t, $^2J_{CP}$ = 6.6 Hz,[31] *o* to PtP), 133.0 (virtual t, $^2J_{CP}$ = 5.9 Hz,[31] *o* to CoP),[29] 130.4 (s, *p* to CoP),[29] 128.5 (virtual t, $^3J_{CP}$ = 5.5 Hz,[31] *m* to PtP), 128.4−128.1 (m, *m* to CoP),[29] 127.5 (virtual t, $^1J_{CP}$ = 30.0 Hz,[31] *i* to PtP), C≡C and Co_2C_2 (2C each) at 106.5 (br s, $w_{1/2}$ = 25.1 Hz), 104.2 (br s, $w_{1/2}$ = 33.2 Hz), 98.8 (s), 91.0 (s), 73.6 (s), 68.1 (s); 29.7 (s, PC*H*$_2$P), 21.3 (s, $C_6H_4CH_3$); $^{31}P\{^1H\}$ 16.8 (s, $^1J_{PtP}$ = 2658 Hz,[32] PtP), 38.6 (br s, CoP).[29]

IR (cm^{-1}, powder film): 2142 (w, $\nu_{C\equiv C}$), 2034/2007/1976 (m/s/s, ν_{CO}). UV−vis (nm (ε, M^{-1} cm^{-1}), 1.25 × 10^{-5} M in CH_2Cl_2): 317 (17 900), 334 (18 300), 359 (17 200). MS:[33] 3313 (M$^+$, 16%), 3143 (M$^+$ − 6CO, 25%), 3087 (M$^+$ − 8CO, 8%), 802 (Pt(P*p*-tol$_3$)$_2$]$^+$, 100%).

***trans*,*trans*-$(C_6F_5)(p\text{-}tol_3P)_2Pt(C{\equiv}C)_8Pt(Pp\text{-}tol_3)_2(C_6F_5)\cdot 2[Co_2(CO)_4(\mu\text{-}PPh_2CH_2PPh_2)]$ (3).** A Schlenk flask was charged with $Co_2(CO)_8$ (0.015 g, 0.047 mmol), $Ph_2PCH_2PPh_2$ (0.016 g, 0.047 mmol), and toluene (5 mL) and fitted with a condenser. The solution was stirred at 65 °C for 4 h. Then a solution of *trans*,*trans*-$(C_6F_5)(p\text{-}tol_3P)_2Pt(C{\equiv}C)_8Pt(Pp\text{-}tol_3)_2(C_6F_5)$ (**PtC$_{16}$Pt**;[8] 0.050 g, 0.023 mmol) in toluene (2 mL) was added. The mixture was refluxed with stirring for 2 h and allowed to cool to room temperature. The solvent was removed by rotary evaporation. The deep red residue was chromatographed on a silica gel column (45 × 3 cm, 10:90 v/v ethyl acetate/hexanes). The solvent was removed from a product-containing fraction by rotary evaporation and oil pump vacuum to give **3** as a deep red solid (0.0054 g, 0.0016 mmol, 7%), mp 251 °C (capillary).

$^{31}P\{^1H\}$ (δ, $CDCl_3$, major signals): 17.6 (s, $^1J_{PtP}$ = 2639 Hz,[32] PtP), 39.8 (br s, CoP).[29] IR (cm^{-1}, powder film): 2131/2084 (w/w, $\nu_{C\equiv C}$), 2003/1976 (s/s, ν_{CO}). MS:[33] 3369 (M$^+$, 1%), 3193 (M$^+$ − 6CO, 3%), 3164 (M$^+$ − 7CO, 1%), 3136 (M$^+$ − 8CO, 2%), 802 (Pt(P*p*-tol$_3$)$_2$]$^+$, 100%).

Crystallography. Complex **1** was dissolved in CH_2Cl_2 and layered with hexane. After 4 days, dark red needles of **1**·$(CH_2Cl_2)_{0.5}$(THF) had formed.[35] Data were collected with a Nonius KappaCCD area detector as outlined in Table 1. Cell parameters were obtained from 10 frames using a 10° scan and refined with 24 248 reflections. Lorentz, polarization, and absorption corrections[36] were applied. The space group was determined from systematic absences and subsequent least-squares refinement. The structure was solved by direct methods. The parameters were refined with all data by full-matrix least-squares on F^2 using SHELXL-97.[37] Non-hydrogen atoms were refined with anisotropic thermal parameters. The hydrogen

(29) The CoPPh$_2$C*H*$_2$PPh$_2$Co ^{1}H NMR signals, the CoP*Ph* ^{13}C NMR signals, and the Co*P*Ph$_2$CH$_2$*P*Ph$_2$Co ^{31}P NMR signals were assigned by analogy to closely related dicobalt complexes.[18b]

(30) The C_6F_5 ^{13}C NMR signals were not observed.

(31) The *J* values given for virtual triplets represent the *apparent* couplings between adjacent peaks and not the mathematically rigorously coupling constants. See: Hersh, W. H. *J. Chem. Educ.* **1997**, *74*, 1485.

(32) This coupling represents a satellite (d; ^{195}Pt = 33.8%) and is not reflected in the peak multiplicity given.

(33) FAB (3-nitrobenzyl alcohol matrix); *m*/*z* for most intense peak of isotope envelope (relative intensity, %).

(34) The C_6F_5 and ipso PC_6H_5 ^{13}C NMR signals were not observed.

(35) The THF is derived from previous crystallization attempts with the same sample.

(36) (a) *Collect* data collection software; Nonius B. V., **1998**. (b) Scalepack data processing software: Otwinowski, Z.; Minor, W. *Methods Enzymol.* **1997**, *276* (Macromolecular Crystallography, Part A), 307.

(37) Sheldrick, G. M. *SHELX-97, Program for refinement of crystal structures*; University of Göttingen, 1997.

atoms were fixed in idealized positions using a riding model. The ortho and meta carbon atoms of one aromatic ring (C35/C35a, C36/C36a) and the CH_2Cl_2 molecule showed displacement disorder, which refined to 56:44 and 50:50 occupancy ratios, respectively. Scattering factors were taken from the literature.[38]

(38) Cromer, D. T.; Waber, J. T. In *International Tables for X-ray Crystallography*; Ibers, J. A., Hamilton, W. C., Eds.; Kynoch: Birmingham, England, 1974.

Acknowledgment. We thank the German-Israel Foundation (GIF, I-883.144.5), the U.S. National Science Foundation (CHE-0719267), and Johnson Matthey (platinum loans) for support, and Professor F.-E. Hong (National Chung-Hsing University) for helpful discussions.

Supporting Information Available: A CIF file with crystallographic data for **1**·$(CH_2Cl_2)_{0.5}$(THF). This material is available free of charge via the Internet at http://pubs.acs.org.